ANALYSIS OF THE DEPTH-DIAMETER RELATIONSHIP OF MARTIAN CRATERS

A Capstone Experience Thesis

Presented by

Jared Howenstine

Completion Date:
May 2006

Approved By:

Professor M. Darby Dyar, Astronomy

Professor Christopher Condit, Geology

Professor Judith Young, Astronomy

Abstract

Title: **Analysis of the Depth-Diameter Relationship of Martian Craters**
Author: **Jared Howenstine, Astronomy**
Approved By: **Judith Young, Astronomy**
Approved By: **M. Darby Dyar, Astronomy**
Approved By: **Christopher Condit, Geology**
CE Type: **Departmental Honors Project**

Using a gridded version of maritan topography with the computer program *Gridview*, this project studied the depth-diameter relationship of martian impact craters. The work encompasses 361 profiles of impacts with diameters larger than 15 kilometers and is a continuation of work that was started at the Lunar and Planetary Institute in Houston, Texas under the guidance of Dr. Walter S. Keifer. Using the most 'pristine,' or deepest craters in the data a depth-diameter relationship was determined: $d = 0.610D^{0.327}$, where d is the depth of the crater and D is the diameter of the crater, both in kilometers. This relationship can then be used to estimate the theoretical depth of any impact radius, and therefore can be used to estimate the pristine shape of the crater. With a depth-diameter ratio for a particular crater, the measured depth can then be compared to this theoretical value and an estimate of the amount of material within the crater, or fill, can then be calculated. The data includes 140 named impact craters, 3 basins, and 218 other impacts. The named data encompasses all named impact structures of greater than 100 kilometers in diameter. In addition to the named impact structures a cursory study of Quasi-Circular Depressions, QCDs, was made. These are theorized impact structures that have been almost completely filled in. The data include 22 of these structures. In addition to the development of the depth-diameter relationship of craters on Mars, a cursory look into results relating to Gusev Crater, three major impact basins, QCDs, and gravity modeling will be discussed.

1. Introduction & History

Throughout the history of planetary astronomy, impact structures have served a very important purpose. Initially, impact structures were studied to date the surface of extraterrestrial bodies, if only in a relative manner, by observing crater density, morphology, or freshness. Again, impact structures will be used to remotely study other planets. The research conducted here began during the summer of 2004 at the Lunar and Planetary Institute in Houston, TX, under the guidance of Dr. Walter Kiefer[1]. The following study is a detailed analysis of the depth to diameter relationship of impact structures on Mars, focusing on impacts larger than 20 km. In this study, 361 impact structures ranging from 17 km up to 2,250 km in diameter were measured using *Gridview* [*Roark et al*., 2002],[2] an IDL application developed by James Roark[3]. This study will show how a depth-diameter relationship of $d = 0.610D^{0.327}$ is produced; where d is the depth in kilometers and D is the diameter in kilometers. This relationship will be used to estimate the potential fill that is present in impacts on the surface of Mars. In addition to the relationship produced, Gusev Crater will be singled out and implications of the relationship with respect to the large impact basins and Quasi-Circular Depressions [*Frey et al*., 2002],[4] QCDs, on Mars will be carried out.

Historically, the study of impact craters began with observations of the Moon by counting the number and measuring the diameter of craters and comparing those data to the ages of returned lunar samples. This method of crater counting was used extensively

---

[1] Dr. Walter Kiefer is a staff scientist at the Lunar and Planetary Institute in Houston, TX. Dr. Kiefer studies Planetary Geophysics. His biography and publications can be found at: http://www.lpi.usra.edu/science/kiefer/

[2] *Gridview* was attained through the website: http://denali.gsfc.nasa.gov/gridview/index.html, with permission by Jim Roark.

[3] James Roark is a system administrator and software engineer at the Planetary Geodynamics Laboratory, NASA Goddard Space Flight Center.

[4] QCDs were initially proposed by Dr. Herbert Frey who is currently working as Chief, Planetary Geodynamics Laboratory, NASA/Goddard Space Flight Center.

on Mars by *Tanaka* [1986] and others. In addition to being studied for relative ages of the surface of solid bodies, impact structures were also of great interest in terms of their mechanisms. *R. J. Pike* [1977] studied impact structures on the Moon, and deduced a correlation between the diameter of impacts and their depth. He measured the diameters and depths of impact structures on the Moon and was able to extract a depth-diameter relationship for the craters that he studied. From his research, he was able to calculate a power-law relationship. A relationship of this form makes it possible to determine the depth of an impact structure just by measuring the diameter of the crater. A previous study by *Williams and Zuber* [1998] analyzed the depths of basins on the Moon from Clementine data. *Garvin and Frawley* [1998] determined a depth-diameter relationship for impact craters on Mars with diameters less than 100 km in diameter to be $d = 0.25D^{0.49}$. The relationship presented here represents a much larger range of diameters than previously studied.

2. Method & Data Collection

The data collected for this project were gathered using the gridded data provided by J. Roark and used in the *Gridview* program. The source of the topographic data is the NASA Mars Global Surveyor (MGS) mission, and specifically, the Mars Orbiter Laser Altimeter (MOLA). [*Smith et al.*, 2001] The altimetry data collected from this mission in grid form enables the construction of topographic profiles of structures on Mars. The gridded version of the Martian topography used in this study has a horizontal resolution of 64 pixels per degree (930 meters per pixel) and a vertical accuracy of approximately 1-2 m. [*Roark, et al.*, 2004] In total, 361 structures were measured, including the three

major named basins on the surface of Mars and 22 QCDs. The minimum standard deviations for the diameter and depths are larger than the accuracy of the data itself and so the standard deviations will represent the error in the measurements used in this study. A more rigorous measure of the uncertainty would be to use the p-test, however, due to time constraints only the standard deviation was calculated. The minimum standard deviation of the depth measurements was 93 m. The minimum standard deviation of the diameter measurements was 963 m, with most significantly larger than this.

Each structure studied required a minimum of four diameter measurements and eight depth measurements, with two depths associated with each diameter measurement. In this study the diameter is a measurement from one point on a crater's rim to another, with a direct line through the center of the crater. The point on the rim is selected for its relative height compared to the rest of the crater rim. The highest elevation, and therefore least eroded point, was selected to provide the maximum depth measurement. Depths were measured on both side of the diameter. The high point on each side of the diameter measurement was measured, and an average was taken. This implicitly means that he resulting relationship will be a low end estimate due to craters that have highly degraded rims for only one section. The reason for this was that it was observed during data collection that there were many crater rims that appeared artificially high due to other near-by impacts, regional topographic slopes, or volcanoes. To off-set these high data points the low end points were also measured. The depth of the crater is a rim-to-floor depth. Each diameter measurement created a topographic profile of the crater. From this profile, the two rim-to-floor depths could be measured.

Within the program, cross-sections can be produced, and from these, the depth and diameter can be measured. The cross-sections were taken by drawing profile lines across the craters. Figure 1 shows a schematic of the process followed to extract depths and diameters from the profiles, and therefore to estimate the fill thickness in the craters. Initially an attempt was made to measure cross sections in a uniform pattern, using cross sections of north-south, northeast-southwest, east-west, and northwest-southeast directions. However, due to the erosion present and the degradation of the impact structures, the cross-sections had to be measured as closely to this as possible, while attempting to retain precise measurements.

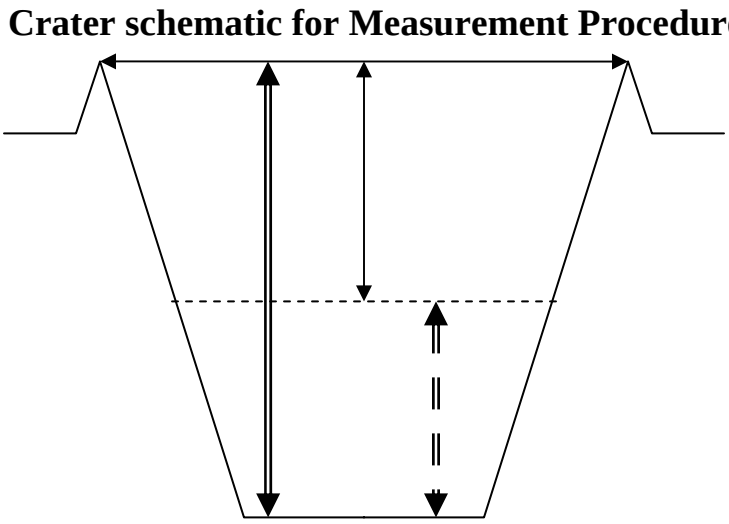

Figure 1. Dashed horizontal line represents the observed fill level. The single horizontal line represents the diameter measurement and the double solid vertical line is the total depth of the crater, unfilled. The single vertical line is the measured depth, and the double dashed vertical line is the depth of fill present.

In total, eight depth measurements were made that were averaged and a standard deviation was calculated to estimate the uncertainty in the measurements. The cross-section part of the program uses the location of the cursor to display a given point's location and elevation. By selecting a particular point, one can draw a line from one location to another. A straight line will output either the diameter with a horizontal line

or the depth with a vertical line. Figure 2 shows a typical direction line and associated profile of a crater.

Due to the nature of the Martian surface, an attempt was made to measure craters in both the Northern and Southern Hemispheres. This is difficult due to the very smooth surface of the northern lowlands. Most impacts in the Northern lowlands are either buried or significantly eroded. Thus, the majority of impact structures studied are located in the southern highlands, where it appears that much less erosion has occurred, and preservation of the structures is significantly better.

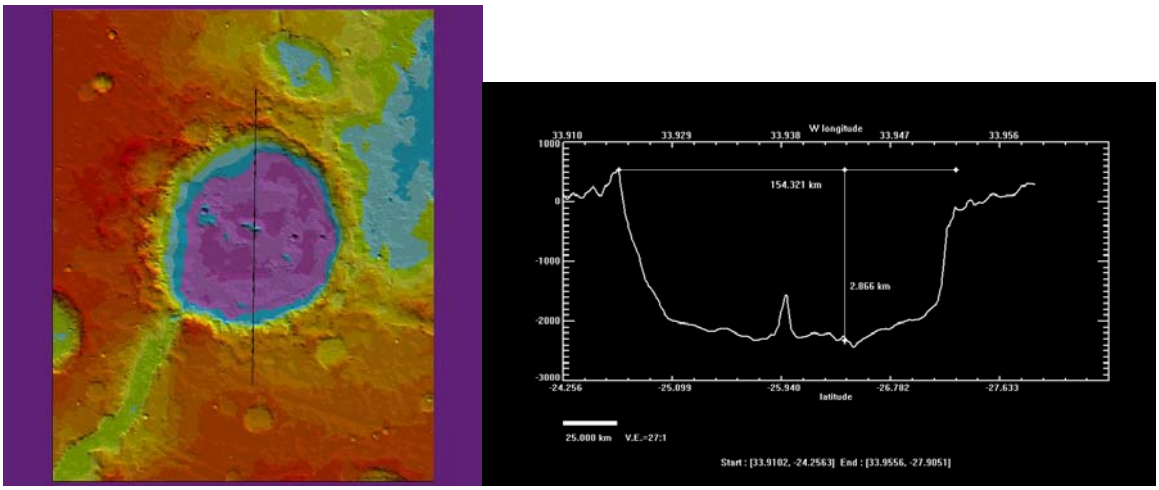

Figure 2. These are representative images from the *Gridview* program. The image on the left is the topographic relief image with a line depicting the north-south profile track. On the right is the north-south profile image, with the lines that are used to measure diameter and depth.

The study began by measuring 39 named impact structures on Mars that had diameters greater than 95 km, see List 1 in the Appendix. [*USGS List*, 2006] The named structures have precisely measured locations on the surface and thus locating and cataloging them was very easy. This also provided a base to work from and allowed the study of known impact structures. After collecting the data for this list, a preliminary depth-diameter relationship was produced.

To calculate the relationship, a proper selection method had to be developed to find the most 'useful' impacts. The impact structures on Mars have a very diverse set of individual depth-to-diameter ratios. This comes from the fill that is present in each crater and the erosion that has taken place. To calculate the relationship presented here the most 'pristine' impact structures in the data were selected. 'Pristine' in this study refers to the deepest craters for a particular diameter range.[5] This, in theory, will provide the least filled, and theoretically unfilled, craters on Mars. These craters are considered unfilled due to the limits of this study and the limits of the knowledge of the Martian surface. Unfortunately it cannot be deduced if there is fill present in the craters, therefore a benchmark for 'pristine' craters had to be set in this study. Figure 3 shows the depth-to-diameter plot of the 39 named structures on Mars that were initially studied. The selected 11 'pristine' craters are highlighted. From these data and the selected points, a depth-to-diameter relationship of $d = 0.44D^{0.38}$ was found. [*Howenstine and Kiefer*, 2004] The relationship was produced from a best-fit power-law tool in Microsoft Excel. A power-fit was used to match the physical relationship, based on the work of Pike. [*Pike*, 1977]

This preliminary relationship allowed a comparison of the initial results to *Garvin and Frawley's* [1998] results, as will be discussed in the analysis of this work. After the comparison, which provided a preliminary check for the initial research, the data collection continued with an additional 101 named craters that are larger than 100 km in

[5] In this study all craters are assumed to be bowl-shaped, particularly for depth measurements. As such, this study assumes simple crater shape, however, on the Moon large craters are observed to have more complex structures such as: central peaks, rings, and peak rings. [Christensen and Hamblin, 1995, p. 78-86] Craters of different sizes have different morphologies, as has been extensively studied for the Moon. [*Pike* 1977, *Kiefer* 2001] The Martian cratering record can be seen in *Strom et al.'s* [1992] work.

diameter, 3 impact basins, 196 unnamed structures, and 22 QCDs.[6] The total data can be seen in the Appendix, where the name or location of the impacts is shown with each depth, diameter, and respective standard deviation in the measurements. The standard deviation was calculated using Microsoft Excel's standard deviation function for the data points.

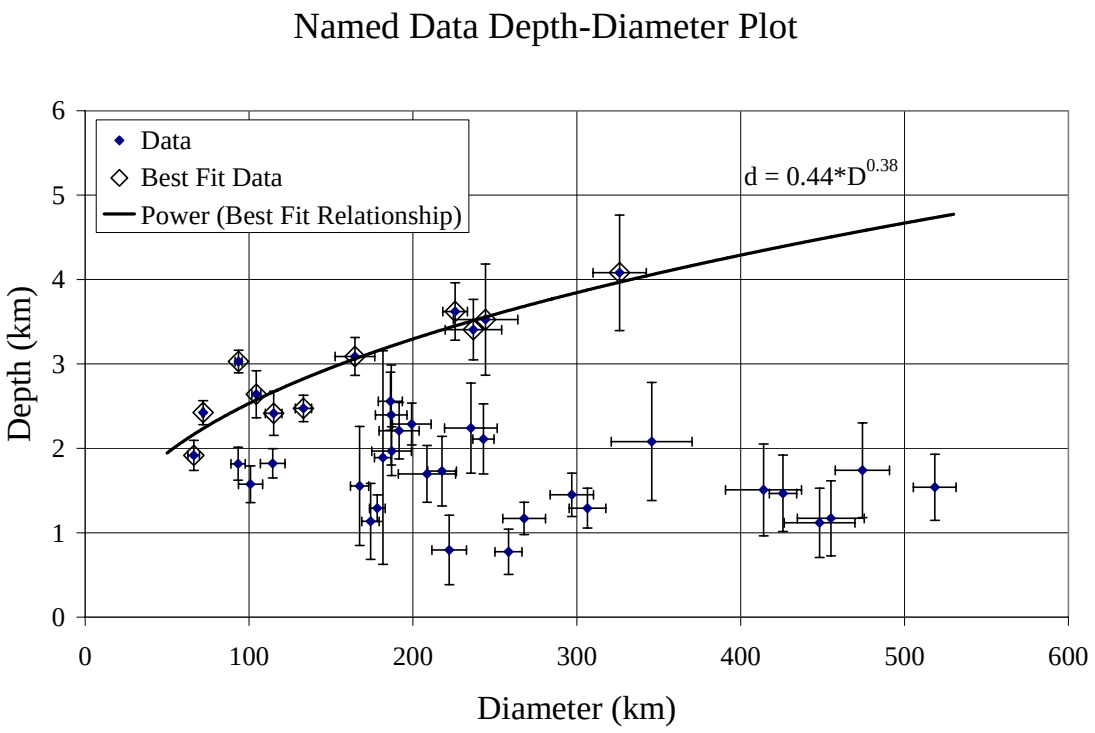

Figure 3. This is the depth-diameter plot of the 39 named structures on Mars that were initially studied. The Best Fit Data are marked with diamonds, and consist of 11 data points. The relationship extracted from these points is: $d = 0.44D^{0.38}$. Error bars are 2 standard deviations.

Quasi-Circular Depressions, or QCDs, were briefly studied in this research. QCDs are hypothesized to be nearly filled impact structures. [*Frey et al.*, 2002] A list of potential QCDs was provided by Dr. Frey through personal correspondence and some others being located from his multi-ring basin work in 1990. [*Schultz and Frey*, 1990]

[6] A few craters from the USGS list that are greater than 100 km in diameter were not cataloged in this study due to the inability to properly profile them. The conclusion here was that some of these impacts are either so eroded or damaged that they do not represent a crater in the topographic data.

The list consisted of the locations of the structures and their potential diameters. This study profiled 22 QCDs that ranged from about 200 km in diameter to a diameter of just under 640 km. These profiles were taken to provide a method on how to approach the issue of QCDs in future work and demonstrate their significant fill. See the Appendix List 4 for a list of the studied QCDs.

The last set of data collected consisted of profiles of the three major basins on Mars: Hellas, Argyre, and Isidis. The diameters of these basins were not calculated in this study, but taken from *Schultz and Frey's* [1990] multi-ring basin work. Unlike the previous method, the depths were measured more than four times each to minimize error. From this, an average depth and standard deviation could be calculated. These data points were never used to actually calculate a power-fit to the data because the study of these was for purely observational purposes. The measured depths and their associated deviations are shown in the Appendix List 1.

3. Analysis

The first stage of analysis entailed an initial comparison to *Garvin and Frawley's* [1998] work. From there, an analysis of the complete set of data collected for a formal depth-to-diameter relationship for the impact structures profiled in this study could be carried out. The range of diameters studied was 17 km up to 518 km, along with a measurement of the depths of the large impact basins. The QCDs measured ranged from 195 km to 639 km in diameter. Once a quantitative relationship between depth and diameter was established, the depth of fill in a particular diameter crater could be calculated. From the depth, the volume of the fill could then be calculated, and in

conjunction with gravity modeling, the density could be extracted. The work conducted here goes as far as developing the relationship for the depth and diameter, and an initial calculation of the depth of fill in the studied craters.

An initial analysis of 39 named impact structures on Mars provided a preliminary depth-diameter relationship. This was calculated to be: $d = 0.44D^{0.38}$, where d is the unfilled depth of the crater in kilometers and D is the diameter measured in kilometers. The range of diameters studied here was from 66 km to 326 km. As discussed above, the most 'pristine' structures were used for the best fit. In this data set, there were 11 craters that fit the definition of 'pristine' that is defined in this study; this being the deepest craters for a given diameter. This relationship is shown in Figure 4 along with the data points that defined it. Also in this image is *Garvin and Frawley's* [1998] relationship of $d = 0.25D^{0.49}$. For the range of overlap between the two sets of data, from 66 to 98 km, the difference between the curves is small (214 m at 66 km and 149 m at 98 km). These misfits are actually within the error associated with the data collected in this research, which implies good correspondence between the two relationships. [*Howenstine and Kiefer*, 2004]

The majority of the impacts studied are located in the southern highlands. There appears to be much less degradation to the structures, and therefore the more pristine impacts are located there. In addition to this, the study of impact craters has shown that larger impacts are generally older. From crater densities, collected by counting the number of crater per area, allow one to determine that the surface of the northern lowlands is significantly younger than the surface of the southern highlands. Because the northern lowlands are younger, they will contain fewer large impacts. Also, due to the

erosion and potential sediment fill, there will be fewer pristine impacts. These factors mean that most impacts are in the Southern Highlands. However, due to the relatively smooth surface of the Northern Lowlands, those impacts that are present appear to be very 'pristine.' These initial data show that an overwhelming majority of the craters do have significant fill present in them, as was proposed initially in this study (see the Appendix for depth anomalies, or the amount of fill present). The potential levels of fill can be extracted from the difference between the measured depth of the crater and the corresponding depth value as calculated from the depth-diameter relationship.

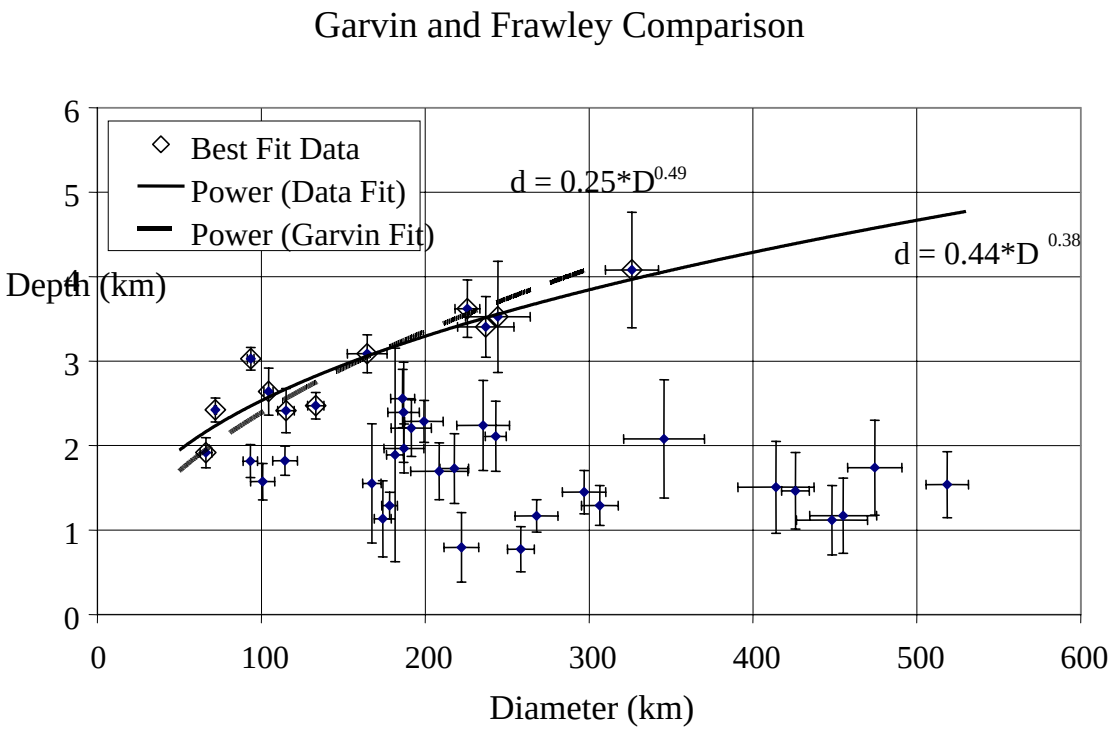

Figure 4. This is Figure 3 shown again, this time showing the comparison between *Garvin and Frawley's* [1998] work and the work presented here. The dashed line is Garvin and Frawley's work and the solid line is the relationship developed in this project. Error bars are 2 standard deviations, based on 8 depth-diameter measurements per crater.

A final compilation of data was next collected. A total of 322 more impacts were measured including the rest of the great then 100 km named impacts and by visually searching the gridded quadrants provided by James Roark. In total there are 140 named

structures, 196 unnamed structures, and 22 QCDs, and 3 basins. From the total data, a depth-to-diameter relationship for impacts on Mars can now be calculated. Figure 5 shows the collected data in a depth-to-diameter plot. As can be seen, there is a large majority of structures that have low depth-to-diameter ratios. Again, the selection of 'pristine' structures from the collected data had to be carried out. These data points are shown in Figure 5 and in the Appendix. These points were selected by choosing those craters with maximum depth among surrounding points of similar diameter. As can be seen in Figure 5, very few large impacts are pristine. This is most likely due to the relative age of these impacts, as they may be so old that erosive and deposition processes have filled in and reduced the depth-diameter relationships of these impacts.

The resulting power fit was $d = 0.610D^{0.327}$, as shown in Figure 5, and determined from the 24 'pristine' craters in the data.[7] A power-law fit allows one to compare points below the curve to the curve itself, and then to determine the loss in depth due to fill. With the diameter and depth, the volume of fill can be determined.[8] This, along with gravity modeling, will be further researched by Dr. Walter Kiefer. The depth of fill for all of the craters studied is shown in the Appendix.

The fill data detail the significance of the depth and quantity of deposits present in impact structures on Mars. In addition to the general study of the impacts on Mars, a profile of Gusev Crater was created to highlight current events and the Spirit Rover Mission. Also, using an extended plot of the relationship that has been determined, a projection out to the diameters of three major basins was used to observe how they fall in

[7] Points above the line, those on the lists with negative fills, empirically means that they have negative fills. However, this may just be an artifact of the best-fit, or, due to the error associated with the measurements, these points may in fact fall within the relationship.

[8] Circles are assumed, however, a discussion of oblique impacts can be found in *Herrick and Forsberg-Taylor* [1993].

relation to this relationship.[9] Finally, observations were made to lay the groundwork for future studies of QCDs.

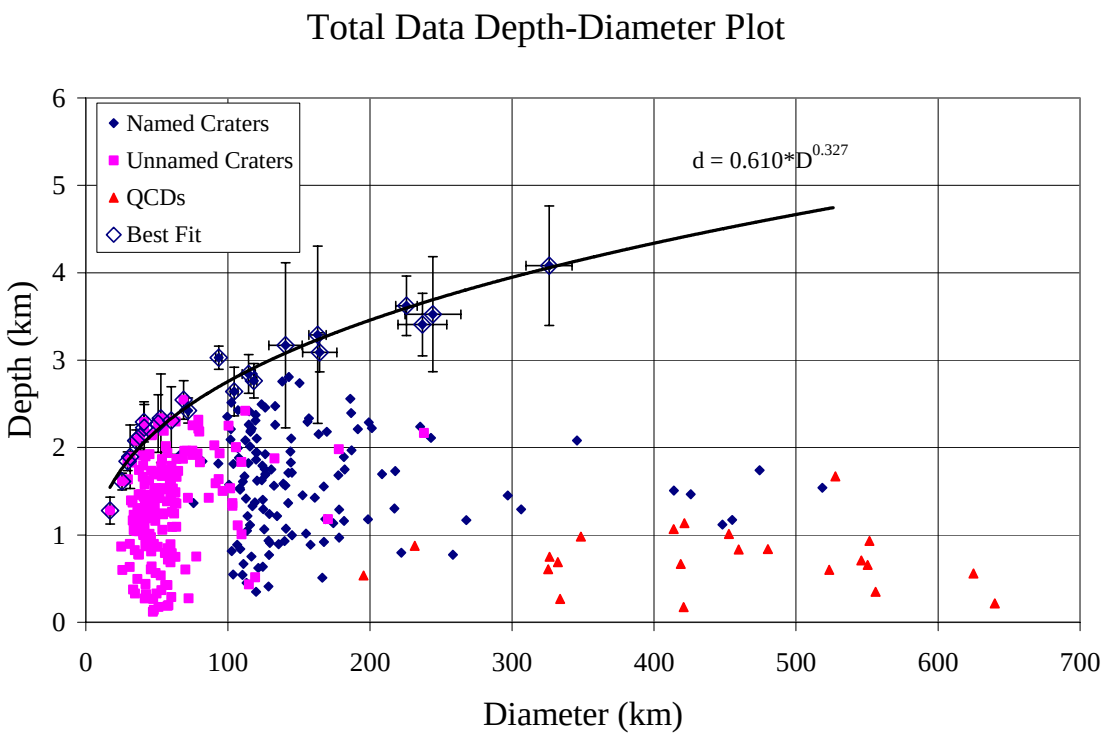

Figure 5. Total data collected as presented in a depth-diameter plot. The only data not shown here is the large impact basin data. The points that show their associated uncertainties are the 24 points used for the best-fit to reduce the clutter in the image. The relationship that is produced is: $d = 0.610D^{0.327}$. Error bars are 2 standard deviations.

4. Observations & Future work

Gusev crater was profiled and singled out so that the potential fill thickness could be calculated. With Mars Exploration Rover Spirit roaming the floor of Gusev crater, this has relevance in terms of current and future work. The rover has studied the composition of the immediate surface material.[10] From this analysis one can make predictions, based on the fill thickness developed here, about the gravity anomaly that

[9] Central Peaks, Peak Rings, and Multi-rings are all ignored as they go beyond the scope of this project.
[10] Analysis of Spirit Rover results can be found in: *Monders et al.* [2006], *Gellert et al.* [2006], *Morris et al.* [2004], and *Lane et al.* [2004].

would be present due to a uniform composition. This can then be compared to the observed gravity anomaly to see if there is a correspondence between what is found at the surface and the total fill. If the gravity anomaly matches the predicted model, then it can reasonably be assumed that the composition is similar throughout. However, if there is a variation in the gravity anomaly when comparing the modeled value and the observed value, then certain changes in possible compositions of the total fill, such as deeper layers that consist of different types of fill, can be made.

Figure 6 shows the plane-view of Gusev from the MOLA data as displayed in the *Gridview* program. Figure 6 also shows a characteristic *Gridview* profile of Gusev that was used in the data collection. From the calculated relationship and using a diameter of 167.477 km, one can determine the 'pristine' depth of Gusev crater as 3.255 km. The actual measured depth of Gusev crater, as measured in this study, is 1.554 km ± 0.705. The power-law fit derived in this study indicates that the depth of fill present in Gusev Crater is between 0.971 and 2.411 km. Even at the low end of the estimate for fill, it is still a significant amount. This fill may come from a sedimentary source that is originating from Ma'adim Vallis to the south of the crater, and cuts through the crater wall on the southern rim. [*Cabrol et al.,* 2003] Another possible source would be volcanism. [*Martinez-Alonzo et al.,* 2005]

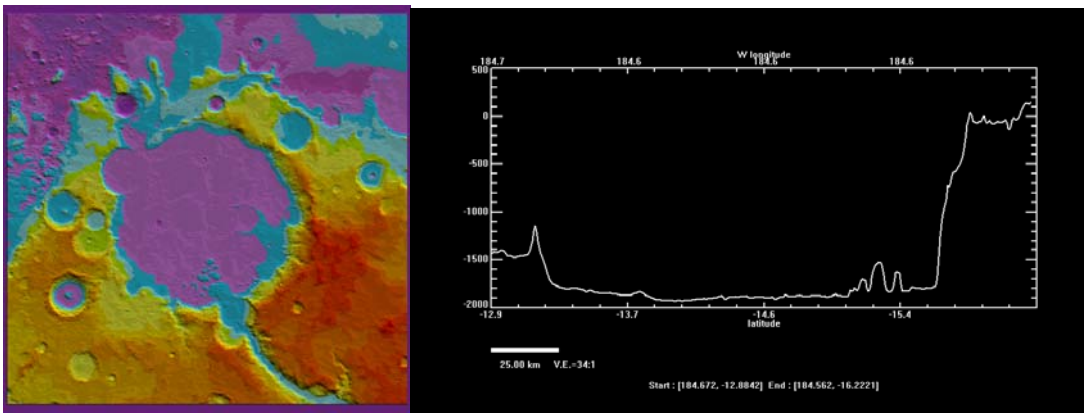

Figure 6. Gusev crater in plain view and topographic profile (north-south). The crater floor is at -1900 meters, the north rim (to the left) peaks at -1100 meters, the south rim (to the right) peaks at approximately 100 meters.

Although the large basins were not used in this study of the depth-diameter relationship, a cursory study of them in this context was carried out. Figure 7 shows the extrapolation of the relationship out to the diameters of the large impact basins on Mars, about 2,250 km. It is observed that the projection matches well with Hellas Basin, which is the largest known basin on Mars.[11] This basin is widely accepted as having a central bulge of fill, but being relatively devoid of fill in comparison to its depth. [*Leonard and Tanaka*, 2001] The other two major basins on Mars, Isidis and Argyre, fall below the line, indicating substantial amounts of fill present. The largest surprise that came from this extrapolation was not that it was shown that fill was present in the basins, but that they actually may fall within this study as a part of the depth-to-diameter relationship for all impacts on Mars.[12] Unfortunately there are only three basins studied here, and so a more thorough study of the large basins may alter this conclusion.[13]

[11] Note that *Shultz and Frey* [1990] have done significant work on identifying other large basins on Mars. The three that are discussed here are the three easiest to identify and measure. Also see *Schultz et al.* [1982] for an earlier study of Martian impact basins.

[12] In this study only one of the rings of the multi-rings basins is measured, and these rings are taken as the primary rings from *Shultz and Frey* [1990].

[13] The three basins studied here are the most visible, and presumably least filled, and will probably have the highest depth-diameter ratios, and so a study of other basins may not alter this conclusion.

This research can be used in the future to help study other impact structures on the surface of Mars. In addition to this, the hope is that, in theory, the extent to which the Martian weathering has been in the past can be better analyzed. This will be shown by the amount of fill that is observed in the vast majority of impact structures on Mars. The volume of fill, as determined from the depth-diameter relationship, will later be used in conjunction with gravity modeling to help determine the density and hopefully the composition of the fills. Detailed gravity modeling will be conducted in the future, but here a cursory study was carried out to test the procedure and observe initial results.

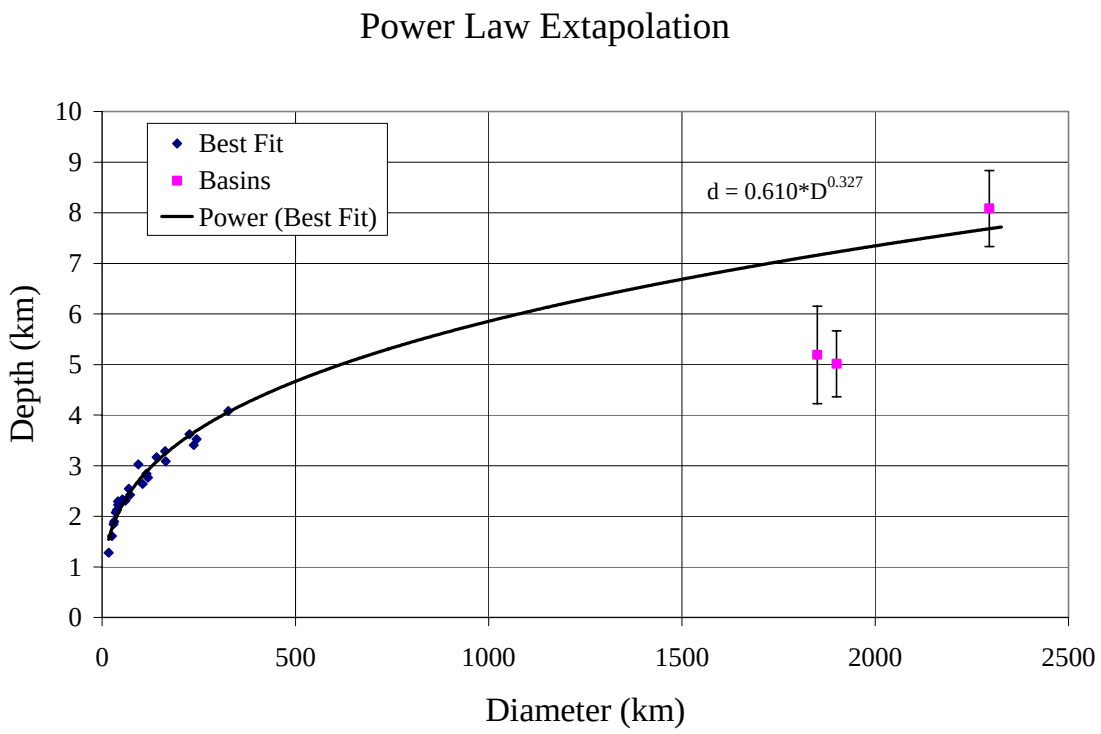

Figure 7. Power-law extrapolation out to diameters of major basins on Mars. Error bars are 2 standard deviations.

The gravity modeling will be conducted by Dr. Kiefer in the near future; however, some initial comments are presented here. The cursory study shows a correlation between the topographic modeling that has been conducted here and some initial gravity models. When comparing similar diameter craters, it is expected that those with more fill

will show larger gravity anomalies. Figure 8a shows the two topographic profiles for the craters Newton and Herschel, 326 km and 297 km respectively, as determined in this study. Figure 8b shows a comparison of the gravity anomalies between the two impacts. As can be seen, the depths, and therefore fill thicknesses, are significantly different for the two craters. Herschel has a shallow rim-to-floor depth of only 1,451 meters with a depth anomaly of 2,475 meters, while the depth of Newton is 4,080 meters with a depth anomaly of -32 meters.

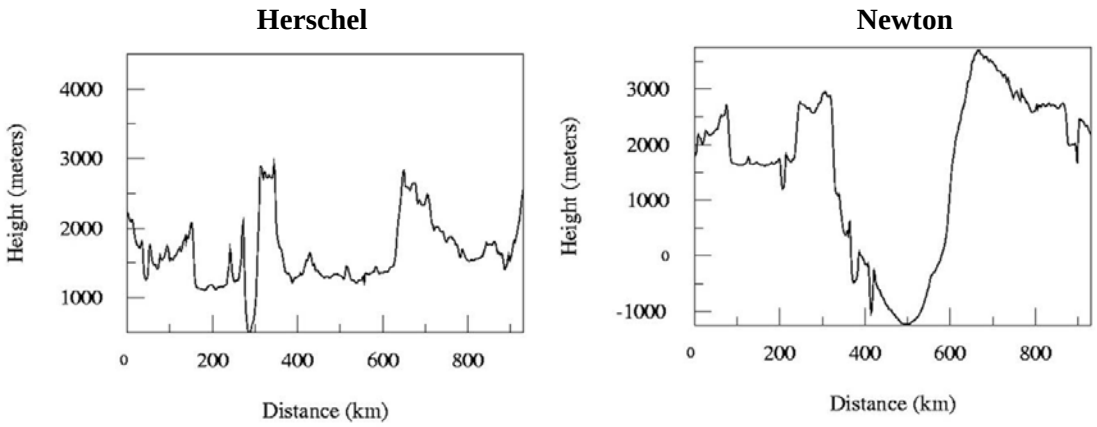

Figure 8a. Topographic profiles of Herschel and Newton craters. Scale has been set to show comparable size of craters, depth range is similar and diameter range is the same.

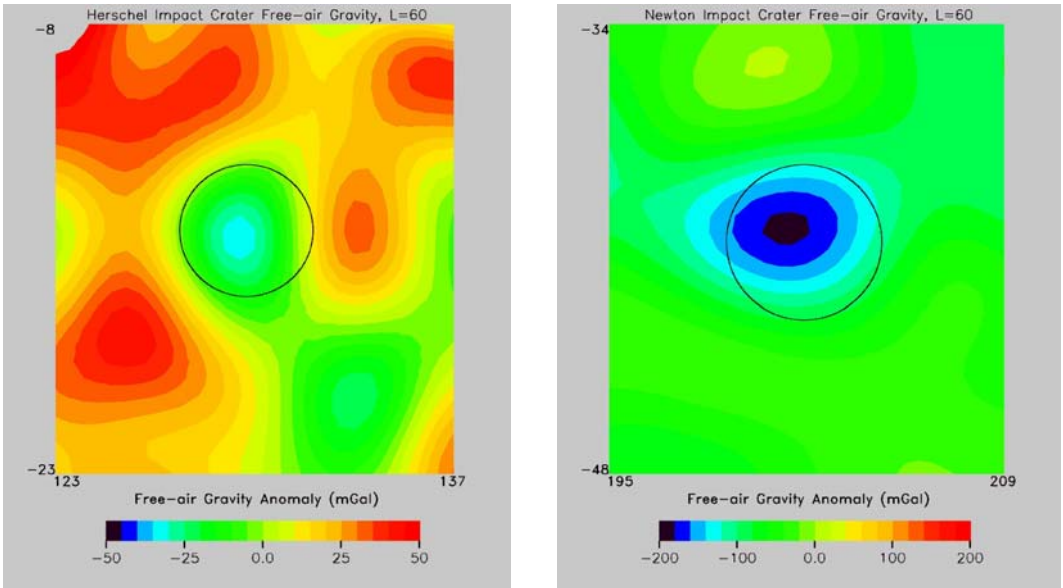

Figure 8b. Gravity profiles of Herschel and Newton impact craters. Gravity anomaly determined from range of values between the center of the low and the approximate crater rim. The crater rim is estimated by the circles, which is a representation of the profiles in Figure 8a.

The Free-air Gravity anomaly modeled for Newton was 170-mGal and for Herschel only 70-mGal was modeled, reflecting the larger amount of fill present in Herschel.[14] The reason for the larger value implying less fill is that this gravity model is looking at the Free-air anomalies. This assumes that the surface is a constant elevation and the values represent the missing material, or holes, so a larger value represents a larger hole in the surface and the deeper crater.

6. Conclusions

Over the course of the past year and a half, the project of profiling and measuring 361 impact structures on the surface of Mars has provided a depth-diameter relationship, allowed for observation of some unexpected but interesting areas for work, and provided the basis for future research. Impact craters hold the key to many aspects of planetary astronomy, whether providing for material to be studied here on Earth by ejecting material into space from the parent body, or giving some indication to the ages of an extraterrestrial object. Even as technology and information improves, craters continue to provide vast amounts of information that can be attained remotely.

The depth-to-diameter relationship that has been developed here is the focus of this project, and was determined to be $d = 0.610D^{0.327}$. From this relationship, the amount of fill in structures can be predicted. With this information, one can predict the depth that should be present given a particular size diameter crater. The combination of the research previously done on the Moon and that which is presented here begins to develop a more comprehensive study of depth-to-diameter relationship for craters in general. When making this connection between the two sets of results, it must be noted

[14] The gravity modeling used here was written and developed by Dr. Walter Kiefer during the summer of 2004 during my internship at the Lunar and Planetary Institute.

that in the present study central peaks, peak-rings, and multi-ring basins are not accounted for, as it goes beyond the scope of this study.

Dr. Kiefer will take this information and further his own research on gravity modeling of impact structures, by estimating the density of the fills, and determining the composition of the fill. Fluvial and aeolian fills will have different densities than fills of volcanic origin and so this determination can be explored using the data provided. In addition to determining the fill of the impacts studied, this information will provide further help to the study of large impact basins and QCDs. This project provides a stepping stone for much future work and presents a depth-diameter relationship for impacts on Mars.

Appendix

List 1. 39 initial named impact structures, used for preliminary results. [*USGS List*, 2006]
* - used in Initial Best-fit, ** - used for Initial and Final Best-fits

Name	Diameter (km)	Standard Deviation (Diameter) (km)	Depth (km)	Standard Deviation (Depth) (km)	Expected Depth (km)	Depth Anomaly (km)
Agassiz	114.440	7.517	1.823	0.173	2.874	1.051
Antoniadi	414.006	23.222	1.508	0.543	4.376	2.869
Bakhuysen**	164.609	12.091	3.088	0.224	3.237	0.149
Baldet	186.250	7.340	2.558	0.344	3.370	0.812
Cassini	425.891	8.377	1.466	0.452	4.417	2.951
Darwin	187.018	12.126	1.968	0.289	3.375	1.407
Dawes	199.258	11.766	2.287	0.249	3.445	1.158
Fesenkov	93.302	4.346	1.818	0.194	2.688	0.870
Flaugergues	267.904	12.979	1.169	0.192	3.796	2.627
Galle**	244.312	19.664	3.525	0.658	3.683	0.158
Green	191.542	12.225	2.210	0.335	3.401	1.192
Gusev	167.477	5.596	1.554	0.705	3.255	1.701
Herschel	296.994	13.250	1.451	0.257	3.926	2.475
Huygens	474.315	16.564	1.740	0.561	4.575	2.835
Kaiser	217.764	8.725	1.730	0.412	3.547	1.817
Kepler	243.011	6.441	2.111	0.415	3.676	1.565
Ladon[15]	518.483	12.972	1.539	0.391	4.710	3.171
Lockyer**	71.957	0.622	2.423	0.143	2.469	0.047
Lomonosov*	133.213	4.928	2.473	0.156	3.020	0.547
Lowell**	236.921	17.173	3.407	0.358	3.646	0.240
Lyot**	225.717	7.531	3.622	0.340	3.589	-0.033
Martz	100.870	7.334	1.574	0.216	2.758	1.184
Mie**	104.418	2.741	2.641	0.278	2.789	0.149
Milankovic*	115.031	5.041	2.416	0.263	2.879	0.463
Mola Hole[16]	455.040	20.415	1.171	0.444	4.513	3.343
Molesworth	178.267	4.755	1.291	0.158	3.322	2.031
Newcomb	258.384	8.268	0.774	0.267	3.751	2.977
Newton**	326.144	16.265	4.080	0.685	4.048	-0.032
Pettit**	93.539	2.093	3.028	0.134	2.691	-0.338
Phillips	186.782	9.631	2.395	0.593	3.373	0.978
Schiaparelli	448.181	21.660	1.118	0.409	4.491	3.373
Schmidt	208.540	17.425	1.697	0.337	3.497	1.800
Schroeter	306.513	11.174	1.292	0.235	3.966	2.675
Secchi	235.384	16.069	2.239	0.533	3.638	1.399
Stoney	174.129	5.226	1.134	0.450	3.297	2.162
Terby	181.638	5.124	1.891	1.265	3.343	1.452

[15] Ladon is a Basin that is cataloged by *Schultz and Frey* [1990] in their basin work. The diameter here is an observed topographic rim as measured in this study, and represents only one of the rings of this potential multi-ring basin.

[16] The Mola Hole is a multi-ring basin that was discovered by *Frey et al.* [*Geophys. Res. Lett.*, 1999 and *Lunar and Planet. Sci. XXX*, 1999]. The diameter here is an observed topographic rim as measured in this study, and represents only one of the rings of this potential multi-ring basin.

Name	Diameter (km)	Standard Deviation (Diameter) (km)	Depth (km)	Standard Deviation (Depth) (km)	Expected Depth (km)	Depth Anomaly (km)
Tikhonravov	345.715	24.646	2.081	0.700	4.126	2.045
Vinogradov	222.140	10.562	0.796	0.412	3.570	2.774
Wahoo*	66.222	3.540	1.917	0.178	2.403	0.487
Hellas Basin	2295	N/A	8.083	0.752	7.661	-0.421
Argye Basin	1850	N/A	5.190	0.963	7.140	1.950
Isidis Basin	1900	N/A	5.014	0.651	7.202	2.189

List 2. 101 additional named impact structures. This completes the named list for all named impact structures larger than 100 km as determined by the USGS. [*USGS List*, 2006]
* - used in Final Best-fit.

Name	Diameter (km)	Standard Deviation (Diameter) (km)	Depth (km)	Standard Deviation (Depth) (km)	Expected Depth (km)	Depth Anomaly (km)
Arago	166.422	4.282	0.509	0.345	3.248	2.739
Arkhangelsky	133.263	11.033	2.259	0.227	3.021	0.762
Arrhenius	129.098	3.725	1.240	0.222	2.990	1.750
Barabashov	129.539	6.867	0.908	0.174	2.993	2.085
Barnard	123.645	4.602	2.495	0.180	2.948	0.453
Becquerel	169.580	3.817	2.181	0.192	3.268	1.087
Bernard	140.853	9.963	1.072	0.235	3.076	2.004
Boeddicker	115.537	2.485	2.013	0.191	2.883	0.870
Bond	119.371	4.701	2.307	0.408	2.914	0.607
Bouguer	113.337	3.570	1.049	0.226	2.865	1.816
Burroughs	112.268	2.536	2.081	0.218	2.856	0.775
Burton	123.897	1.528	1.627	0.229	2.950	1.323
Byrd	128.988	4.771	0.770	0.465	2.989	2.218
Campbell	132.414	3.440	1.562	0.313	3.014	1.452
Cerulli*	118.303	2.058	2.763	0.197	2.905	0.142
Chamberlin	120.377	6.963	1.942	0.396	2.922	0.980
Charlier	108.496	6.448	1.518	0.241	2.824	1.306
Coblentz	110.194	13.038	0.543	0.238	2.839	2.296
Columbus	119.779	2.151	1.942	0.181	2.917	0.975
Comas Sola	124.274	6.856	1.793	0.225	2.953	1.159
Crommelin	120.503	5.768	1.621	0.194	2.923	1.302
Curie*	114.609	4.586	2.842	0.221	2.875	0.034
Da Vinci	102.666	1.916	0.814	0.251	2.774	1.959
Dejnev	154.950	9.292	1.016	0.604	3.173	2.158
Denning	167.632	8.248	0.921	0.246	3.256	2.335
Du Martheray	102.085	0.963	2.211	0.863	2.769	0.558
Flammarion	177.736	18.845	1.683	0.574	3.319	1.636
Fournier	119.845	3.814	1.861	0.248	2.918	1.056
Gale*	163.122	6.095	3.289	1.014	3.227	-0.062
Galilaei	145.065	8.886	1.711	0.237	3.106	1.394
Gilbert	124.777	6.222	1.296	0.329	2.956	1.660

Name	Diameter (km)	Standard Deviation (Diameter) (km)	Depth (km)	Standard Deviation (Depth) (km)	Expected Depth (km)	Depth Anomaly (km)
Graff	158.187	7.151	0.888	0.184	3.195	2.307
Hadley	121.383	4.724	0.623	0.290	2.930	2.307
Hale*	140.555	11.751	3.169	0.944	3.074	-0.095
Hartwig	106.972	7.272	1.993	0.092	2.811	0.819
Helmholtz	120.314	7.894	2.102	0.272	2.921	0.819
Henry	201.309	7.258	2.221	0.304	3.457	1.236
Holden	157.004	6.162	2.333	0.585	3.187	0.854
Holmes	115.537	3.377	1.114	0.304	2.883	1.769
Hooke	144.546	4.430	2.103	0.901	3.102	0.999
Huxley	112.645	6.450	1.417	0.405	2.859	1.442
Janssen	161.110	7.821	1.425	0.417	3.214	1.789
Knobel	130.623	2.673	1.749	0.586	3.001	1.253
Krishtofovich	108.622	5.996	0.839	0.502	2.825	1.986
Lasswitz	111.639	2.350	1.669	0.296	2.851	1.182
Lau	113.148	7.903	0.453	0.286	2.863	2.411
Le Verrier	142.472	5.136	1.364	0.263	3.087	1.723
Li Fan	110.476	1.746	1.609	0.260	2.841	1.233
Liais	126.349	6.448	1.688	0.427	2.969	1.281
Liu Hsin	144.279	4.492	1.829	0.447	3.100	1.271
Lohse	150.393	8.521	2.737	0.214	3.143	0.406
Lyell	139.046	17.146	1.585	0.398	3.063	1.478
Madler	135.668	9.092	0.896	0.260	3.038	2.143
Magelhaens	106.563	2.014	0.886	0.157	2.808	1.921
Maggini	145.128	8.913	0.996	0.288	3.106	2.110
Main	111.011	9.644	0.669	0.193	2.846	2.177
Maraldi	119.544	6.576	2.373	0.367	2.915	0.542
Mariner	168.606	3.572	1.180	0.668	3.262	2.083
Maunder	99.570	6.014	2.352	0.215	2.746	0.394
Mellish	103.719	4.985	0.547	0.212	2.783	2.236
Millochau	118.994	2.087	1.371	0.331	2.911	1.540
Mitchel	139.895	4.197	0.929	0.538	3.069	2.140
Moreux	142.881	5.097	2.807	0.752	3.090	0.284
Muller	125.531	7.453	1.064	0.258	2.962	1.898
Mutch	217.275	8.059	1.301	0.351	3.544	2.243
Nicholson	75.809	4.491	1.365	0.264	2.512	1.147
Oudemans	138.339	7.028	2.755	1.348	3.058	0.303
Pasteur	126.301	4.556	2.457	0.208	2.968	0.511
Perepelkin	82.023	6.034	1.843	0.449	2.577	0.735
Peridier	101.833	5.911	2.092	0.224	2.766	0.674
Pickering	119.890	2.769	0.350	0.206	2.918	2.568
Porter	107.113	3.429	2.426	0.378	2.812	0.387
Proctor	181.822	3.741	1.160	0.287	3.344	2.184
Ptolemaeus	178.365	8.980	0.969	0.294	3.323	2.354
Quenisset	143.949	4.430	1.954	0.109	3.098	1.144
Rabe	116.165	4.766	2.193	0.159	2.888	0.695
Radau	115.851	4.269	2.180	0.389	2.886	0.705

Name	Diameter (km)	Standard Deviation (Diameter) (km)	Depth (km)	Standard Deviation (Depth) (km)	Expected Depth (km)	Depth Anomaly (km)
Rayleigh	128.517	14.463	0.934	0.446	2.985	2.051
Roddenberry	140.379	16.896	1.566	0.312	3.073	1.506
Rudaux	113.839	4.504	1.216	0.283	2.869	1.653
Russell	142.535	4.605	1.710	0.214	3.088	1.378
Rutherford	116.778	4.456	2.216	0.214	2.893	0.677
Savich	198.575	9.044	1.178	0.606	3.442	2.264
Schaeberle	163.876	7.176	2.152	0.546	3.232	1.080
Sharonov	102.399	1.735	2.512	0.749	2.771	0.259
Sklodowska	124.525	6.999	0.637	0.265	2.954	2.318
Slipher	128.580	8.940	0.411	0.340	2.986	2.575
South	103.813	2.983	1.813	0.167	2.784	0.971
Steno	108.433	11.026	1.537	0.380	2.824	1.287
Teisserenc de Bort	126.348	10.340	1.697	0.329	2.969	1.271
Tikhov	114.657	7.373	2.261	0.305	2.876	0.615
Trouvelot	155.987	4.684	2.294	0.345	3.180	0.886
Very	116.480	8.218	0.753	0.464	2.891	2.138
Vogel	125.783	5.256	1.755	0.261	2.964	1.210
Wallace	182.215	6.356	1.748	0.500	3.346	1.598
Wells	107.648	6.263	1.883	0.209	2.817	0.934
Wien	124.588	4.921	1.402	0.215	2.955	1.553
Williams	134.583	6.225	1.216	0.325	3.030	1.815
Wirtz	126.286	7.835	1.923	0.235	2.968	1.045
Wislicenus	152.514	10.855	1.454	0.234	3.157	1.703
Wright	117.297	3.301	1.329	0.164	2.897	1.568

List 3. Unnamed impact structures, with listed diameter, depth, associated errors and locations based off of west longitude. List is sorted by diameter.
* - used for Total Best-fit.

#	Diameter (km)	Standard Deviation (Diameter) (km)	Depth (km)	Standard Deviation (Depth) (km)	Expected Depth (km)	Depth Anomaly (km)	Latitude	West Positive Longitude
1*	17.046	0.810	1.279	0.154	1.542	0.263	-27.76	266.64
2	24.952	0.735	0.867	0.074	1.747	0.879	-41.21	292.14
3*	25.419	0.346	1.611	0.096	1.757	0.146	-31.56	271.24
4	25.747	1.074	0.600	0.098	1.765	1.165	-47.32	276.34
5*	29.271	1.234	1.842	0.107	1.840	-0.002	-46.12	238.70
6	29.534	2.303	1.635	0.406	1.846	0.211	-28.35	301.68
7	30.926	1.154	0.633	0.072	1.874	1.241	-30.33	241.08
8	31.056	1.009	0.896	0.137	1.876	0.980	-56.53	309.81
9*	31.225	0.694	1.893	0.363	1.879	-0.014	-32.46	256.93
10	31.527	1.203	1.873	0.486	1.885	0.012	-36.31	273.44
11	31.816	1.762	1.396	0.097	1.891	0.495	-35.67	284.66
12	32.715	1.319	1.827	0.136	1.908	0.082	-35.55	244.51
13	32.895	0.290	1.370	0.148	1.912	0.542	-49.02	306.02
14	33.064	1.714	1.164	0.152	1.915	0.751	-40.99	317.72

#	Diameter (km)	Standard Deviation (Diameter) (km)	Depth (km)	Standard Deviation (Depth) (km)	Expected Depth (km)	Depth Anomaly (km)	Latitude	West Positive Longitude
15	33.283	2.135	0.375	0.087	1.919	1.544	-41.65	318.35
16	33.739	5.270	1.056	0.176	1.928	0.871	-60.17	246.24
17	33.756	0.545	1.231	0.125	1.928	0.697	-57.76	249.05
18	34.181	1.315	1.220	0.311	1.936	0.716	-54.89	263.98
19	34.418	2.297	0.825	0.392	1.940	1.115	-44.16	239.67
20	34.577	1.707	0.328	0.161	1.943	1.615	-28.90	271.13
21*	35.352	1.321	2.077	0.124	1.957	-0.120	-58.86	248.17
22	35.352	1.513	1.156	0.373	1.957	0.801	-49.04	242.03
23	35.453	1.516	1.043	0.086	1.959	0.917	-32.80	297.87
24	36.263	0.651	1.262	0.128	1.974	0.712	-35.81	264.00
25	36.292	2.227	0.497	0.334	1.974	1.478	-42.29	311.74
26	36.540	3.915	1.049	0.341	1.979	0.929	-50.25	258.41
27	36.942	1.341	0.777	0.097	1.986	1.209	-31.05	239.98
28	37.226	1.431	1.186	0.370	1.991	0.805	-47.77	244.56
29	37.345	2.877	1.462	0.368	1.993	0.531	-35.18	314.90
30	37.345	1.907	1.042	0.286	1.993	0.951	-56.69	244.10
31	37.380	1.351	1.459	0.168	1.993	0.534	-31.26	265.77
32	37.428	0.262	1.742	0.111	1.994	0.252	-51.64	244.01
33	37.439	1.096	0.774	0.228	1.994	1.221	-54.54	294.32
34	38.001	3.220	1.307	0.390	2.004	0.697	-56.04	247.09
35*	38.231	0.166	2.124	0.140	2.008	-0.116	-58.98	270.21
36	38.267	1.330	1.219	0.262	2.009	0.789	-30.13	283.86
37	38.947	1.354	1.182	0.196	2.020	0.838	-44.33	276.72
38	38.959	0.676	1.465	0.140	2.020	0.555	-58.23	292.11
39	39.804	1.595	1.910	0.226	2.035	0.124	-35.68	247.97
40	39.976	1.790	1.121	0.193	2.038	0.917	-29.30	315.31
41	40.254	1.519	1.665	0.590	2.042	0.377	-29.84	276.34
42	40.331	0.550	1.793	0.241	2.043	0.250	-48.97	309.97
43	40.401	1.785	1.013	0.534	2.045	1.032	-53.23	241.56
44	40.508	0.921	0.997	0.268	2.046	1.049	-36.59	314.84
45	40.827	1.196	1.440	0.129	2.052	0.612	-31.66	249.77
46	40.845	1.413	1.104	0.269	2.052	0.948	-43.69	257.08
47*	40.939	0.675	2.293	0.229	2.054	-0.239	-54.96	258.53
48	40.945	0.566	1.255	0.202	2.054	0.799	-52.67	307.68
49*	40.998	0.742	2.227	0.266	2.054	-0.172	-54.95	258.54
50	41.271	1.927	1.082	0.118	2.059	0.977	-35.48	254.51
51	41.306	1.280	1.581	0.931	2.060	0.478	-48.00	315.37
52	41.460	1.072	1.253	0.146	2.062	0.809	-53.39	306.85
53	41.466	2.070	0.273	0.276	2.062	1.789	-28.98	268.55
54	41.661	1.617	1.357	0.071	2.065	0.708	-51.15	293.43
55	41.838	1.112	0.869	0.446	2.068	1.199	-52.27	278.29
56	41.951	0.971	0.972	0.147	2.070	1.098	-45.07	281.07
57	41.998	1.409	1.452	0.432	2.071	0.619	-51.90	254.20
58	42.027	1.597	0.439	0.306	2.071	1.633	-35.39	256.97
59	42.086	2.611	1.898	0.118	2.072	0.174	-39.51	241.81
60	42.347	0.572	1.188	0.092	2.076	0.888	-41.12	322.43

#	Diameter (km)	Standard Deviation (Diameter) (km)	Depth (km)	Standard Deviation (Depth) (km)	Expected Depth (km)	Depth Anomaly (km)	Latitude	West Positive Longitude
61	42.347	2.720	1.380	0.448	2.076	0.696	-27.91	262.20
62	42.394	2.855	0.322	0.046	2.077	1.756	-51.59	321.82
63	42.920	3.196	1.227	0.601	2.085	0.859	-43.88	245.72
64	42.938	1.398	1.392	0.275	2.086	0.693	-52.54	259.74
65	43.287	1.580	0.913	0.245	2.091	1.178	-57.40	270.66
66	43.943	1.786	0.897	0.260	2.102	1.204	-57.39	270.64
67	43.979	1.401	1.235	0.734	2.102	0.868	-55.42	300.72
68	44.351	0.847	1.460	0.957	2.108	0.648	-60.79	277.08
69	44.464	0.588	1.623	0.391	2.110	0.486	-41.97	247.48
70	44.558	2.588	1.330	0.768	2.111	0.782	-55.41	300.72
71	44.836	2.776	1.010	0.227	2.115	1.106	-61.13	243.74
72	44.865	3.888	1.925	0.149	2.116	0.191	-48.59	320.96
73	44.937	0.830	1.354	0.142	2.117	0.763	-42.69	321.89
74	45.528	1.107	1.357	0.165	2.126	0.769	-59.01	265.74
75	45.752	1.773	0.605	0.403	2.130	1.525	-39.21	312.22
76	45.971	0.507	0.973	0.413	2.133	1.160	-54.58	286.48
77	46.013	3.579	0.810	0.738	2.133	1.323	-55.42	267.55
78	46.030	2.917	1.734	0.320	2.134	0.400	-33.22	275.67
79	46.373	3.500	1.348	0.543	2.139	0.791	-44.95	315.59
80	46.403	2.798	0.639	0.360	2.139	1.501	-38.85	310.87
81	46.427	1.807	2.141	0.373	2.140	-0.001	-53.28	269.89
82	46.870	1.483	2.149	0.362	2.146	-0.003	-53.31	269.92
83	47.000	0.769	1.328	0.232	2.148	0.820	-30.55	323.24
84	47.077	1.627	1.201	0.082	2.149	0.949	-40.50	328.79
85	47.154	3.525	0.122	0.073	2.151	2.029	-32.45	248.18
86	47.420	1.017	1.314	0.281	2.155	0.841	-57.00	273.35
87	47.503	0.878	0.268	0.329	2.156	1.888	-36.98	241.44
88	47.550	1.397	1.448	0.743	2.157	0.708	-28.84	294.43
89	47.846	2.985	0.141	0.033	2.161	2.020	-30.79	255.45
90	47.863	0.532	0.898	0.362	2.161	1.264	-60.87	309.05
91	47.869	1.472	1.715	0.547	2.161	0.446	-61.75	254.74
92	48.159	1.758	1.526	0.112	2.166	0.639	-53.07	308.03
93	48.602	2.044	1.222	0.065	2.172	0.950	-58.17	278.27
94	48.614	4.810	1.319	0.276	2.172	0.854	-32.38	324.53
95	48.774	1.687	1.692	0.331	2.175	0.483	-42.98	241.10
96	48.857	2.358	1.160	0.076	2.176	1.016	-30.12	315.66
97	49.194	2.431	0.564	0.145	2.181	1.616	-41.57	288.90
98	49.288	2.757	1.712	0.431	2.182	0.470	-29.73	278.74
99	49.430	0.718	1.452	0.107	2.184	0.732	-61.99	321.06
100	49.667	1.897	1.535	0.139	2.187	0.653	-33.89	327.96
101	49.702	4.684	0.328	0.166	2.188	1.860	-51.16	316.22
102	50.222	1.915	1.529	0.087	2.195	0.666	-52.20	323.55
103	50.684	2.208	0.864	0.351	2.202	1.338	-41.43	315.31
104*	50.932	2.619	2.274	0.330	2.206	-0.068	-45.02	317.82
105	51.158	2.543	0.175	0.078	2.209	2.034	-32.29	244.54
106	51.913	3.510	1.420	0.217	2.219	0.799	-56.68	267.62

#	Diameter (km)	Standard Deviation (Diameter) (km)	Depth (km)	Standard Deviation (Depth) (km)	Expected Depth (km)	Depth Anomaly (km)	Latitude	West Positive Longitude
107	52.747	1.880	0.535	0.164	2.231	1.696	-38.95	322.98
108*	52.771	1.478	2.334	0.508	2.231	-0.103	-58.13	255.86
109	52.860	1.885	1.522	0.140	2.232	0.710	-60.33	330.42
110	53.126	3.392	1.789	0.360	2.236	0.448	-48.90	326.21
111	53.191	1.514	0.368	0.129	2.237	1.869	-37.15	257.76
112	53.415	1.339	1.674	0.820	2.240	0.566	-34.31	257.70
113	53.628	0.763	1.866	0.250	2.243	0.377	-29.23	285.56
114	53.717	1.481	1.525	0.202	2.244	0.720	-52.13	326.67
115	53.889	7.634	1.057	0.249	2.247	1.189	-35.28	292.87
116	53.906	1.839	1.245	0.123	2.247	1.002	-57.56	268.77
117	53.971	3.685	1.678	0.689	2.248	0.570	-30.03	286.62
118	54.438	1.710	1.233	0.092	2.254	1.021	-57.56	268.75
119	54.834	1.247	1.532	0.765	2.259	0.728	-51.16	276.33
120	54.953	3.327	2.193	0.137	2.261	0.068	-34.85	322.90
121	55.337	2.708	1.530	0.188	2.266	0.737	-43.29	320.34
122	55.526	1.533	1.751	0.448	2.269	0.518	-59.92	274.87
123	55.603	1.293	0.791	0.303	2.270	1.479	-36.72	278.68
124	55.857	3.507	0.427	0.302	2.273	1.846	-33.55	279.03
125	56.327	2.689	2.016	0.615	2.279	0.264	-35.84	311.33
126	56.425	7.244	1.697	0.266	2.281	0.583	-30.77	326.21
127	57.235	1.627	1.383	0.393	2.291	0.908	-55.85	462.75
128	57.353	2.622	1.935	0.849	2.293	0.358	-37.89	251.12
129	57.442	1.605	0.426	0.284	2.294	1.868	-34.16	281.90
130	57.531	3.603	0.848	0.196	2.295	1.448	-50.85	268.36
131	57.666	3.346	0.189	0.042	2.297	2.108	-33.41	247.77
132	57.738	2.393	0.717	0.241	2.298	1.581	-45.46	269.03
133	58.205	3.817	0.197	0.124	2.304	2.107	-57.90	316.18
134	58.601	2.467	0.812	0.212	2.309	1.497	-38.97	296.51
135	59.198	3.324	1.612	0.415	2.317	0.705	-43.27	329.71
136	59.304	4.406	1.686	1.076	2.318	0.632	-48.17	255.48
137	59.600	0.703	0.891	0.367	2.322	1.431	-58.70	280.16
138	59.600	4.284	0.688	0.205	2.322	1.634	-45.43	269.05
139	59.659	1.120	1.469	0.150	2.323	0.854	-59.40	246.19
140	59.813	1.683	1.496	0.746	2.325	0.829	-53.79	274.59
141	59.960	2.836	1.628	0.295	2.326	0.698	-56.85	281.40
142	59.990	3.405	1.414	0.396	2.327	0.913	-55.42	279.55
143*	60.002	2.260	2.309	0.386	2.327	0.018	-31.91	331.69
144	60.144	4.237	0.290	0.169	2.329	2.039	-38.85	321.17
145	60.368	3.634	1.788	0.234	2.332	0.544	-60.33	267.20
146	60.475	4.783	0.790	0.203	2.333	1.543	-50.88	268.39
147	60.664	2.762	1.264	0.248	2.335	1.072	-47.91	300.84
148	60.812	0.844	1.090	0.222	2.337	1.247	-39.83	320.20
149	61.418	3.636	1.531	0.377	2.345	0.814	-49.92	314.75
150	62.160	1.018	1.245	0.168	2.354	1.109	-30.21	327.61
151	62.580	1.849	1.371	0.338	2.359	0.988	-61.86	266.22
152	63.006	1.912	1.488	0.732	2.364	0.877	-39.50	260.59

#	Diameter (km)	Standard Deviation (Diameter) (km)	Depth (km)	Standard Deviation (Depth) (km)	Expected Depth (km)	Depth Anomaly (km)	Latitude	West Positive Longitude
153	63.024	0.696	0.747	0.429	2.365	1.618	-59.52	271.49
154	63.218	1.133	2.297	0.254	2.367	0.070	-47.41	326.08
155	63.591	0.408	1.092	0.211	2.372	1.280	-37.92	329.45
156	63.763	0.979	1.869	0.138	2.374	0.505	-57.75	241.83
157	63.780	4.506	1.359	0.259	2.374	1.015	-51.79	256.77
158	63.893	2.513	1.663	0.204	2.375	0.712	-59.76	306.11
159	65.037	2.054	1.730	0.464	2.389	0.659	-36.58	318.18
160	68.358	3.164	1.870	0.122	2.428	0.559	-61.71	241.87
161*	68.759	2.596	2.545	0.221	2.433	-0.112	-38.65	247.09
162	69.311	2.311	1.962	0.525	2.439	0.477	-34.41	259.18
163	70.030	2.531	0.604	0.458	2.448	1.844	-55.51	241.94
164	70.952	3.006	1.960	0.189	2.458	0.498	-55.24	274.06
165	71.916	3.666	1.423	0.261	2.469	1.046	-47.93	300.82
166	72.348	4.911	0.274	0.094	2.474	2.200	-61.31	285.92
167	75.025	3.398	1.963	0.685	2.503	0.540	-37.42	326.81
168	75.207	3.597	2.253	0.224	2.505	0.252	-31.26	251.29
169	75.245	2.587	1.915	0.215	2.506	0.591	-58.07	273.65
170	77.740	3.795	0.752	0.442	2.533	1.781	-38.85	309.54
171	78.639	2.147	1.931	0.298	2.542	0.611	-40.67	325.49
172	79.233	0.682	2.317	0.392	2.548	0.232	-34.64	316.34
173	79.245	1.282	2.216	0.801	2.549	0.333	-53.14	272.91
174	79.954	6.286	2.184	0.569	2.556	0.372	-28.89	275.89
175	80.424	1.180	1.830	0.568	2.561	0.731	-49.83	261.02
176	86.491	3.477	1.423	0.258	2.623	1.200	-52.24	249.86
177	90.517	3.075	2.024	0.410	2.662	0.638	-28.59	303.52
178	91.351	3.183	1.591	0.270	2.670	1.079	-59.59	250.92
179	93.480	4.321	1.637	0.116	2.690	1.053	-59.60	250.87
180	94.189	0.806	1.934	0.167	2.697	0.763	-40.93	331.10
181	96.436	1.391	1.501	1.104	2.718	1.216	-30.31	300.85
182	100.566	3.125	2.250	0.253	2.755	0.505	-28.42	310.00
183	101.728	7.623	1.532	1.137	2.765	1.234	-30.44	300.81
184	103.280	3.291	1.332	0.438	2.779	1.447	-31.71	319.03
185	103.295	2.197	1.363	0.814	2.779	1.416	-37.69	310.79
186	105.734	3.314	2.004	1.060	2.801	0.796	-50.08	271.09
187	106.961	1.826	1.109	0.227	2.811	1.702	-50.51	327.95
188	109.503	3.730	1.833	0.234	2.833	1.000	-43.56	325.13
189	109.695	2.560	1.006	0.554	2.834	1.829	-48.12	262.70
190	112.252	5.160	2.420	0.273	2.856	0.436	-50.75	254.23
191	114.824	4.007	0.434	0.178	2.877	2.443	-57.84	307.36
192	119.200	8.510	0.514	0.424	2.913	2.399	-41.22	263.63
193	132.902	13.752	1.874	0.510	3.018	1.144	-37.89	317.39
194	170.506	8.273	1.182	0.230	3.274	2.092	-47.63	330.31
195	178.208	1.193	1.979	0.750	3.322	1.342	-52.49	249.18
196	238.074	13.541	2.166	0.524	3.652	1.486	-57.92	258.24

List 4. List of studied QCDs. Locations not listed to preserve research by Dr. Frey in the future. Names are reference names used in this research.

Name	Diameter (km)	Standard Deviation (Diameter) (km)	Depth (km)	Standard Deviation (Depth) (km)	Expected Depth (km)	Depth Anomaly (km)
004lowlands	195.546	2.964	0.536	0.354	3.424	2.888
016highlands	545.918	6.371	0.708	0.434	4.790	4.082
021lowlands	420.806	2.937	0.174	0.096	4.400	4.226
024misc	527.707	10.461	1.670	0.863	4.738	3.068
029lowlands	555.941	37.753	0.350	0.179	4.819	4.469
051highlands	413.888	13.029	1.067	0.365	4.376	3.309
053lowlands	639.871	12.529	0.218	0.196	5.046	4.828
057highlands	326.439	3.874	0.751	0.234	4.049	3.298
077highlands	348.434	33.983	0.982	0.450	4.136	3.155
083highlands	325.434	6.781	0.608	0.358	4.045	3.437
098highlands	421.456	6.930	1.134	0.291	4.402	3.268
113highlands	624.911	5.429	0.558	0.735	5.007	4.449
165highlands	332.293	5.145	0.689	0.428	4.073	3.384
191highlands	550.471	25.791	0.657	0.164	4.803	4.147
192highlands	523.391	10.207	0.601	0.513	4.725	4.124
195highlands	459.606	22.465	0.835	0.759	4.528	3.693
196highlands	418.855	3.220	0.670	0.318	4.393	3.723
288highlands	480.228	8.365	0.839	0.548	4.594	3.755
300highlands	333.948	9.801	0.268	0.385	4.079	3.811
352highlands	551.653	19.056	0.932	1.421	4.807	3.875
356highlands	231.452	15.048	0.875	0.509	3.618	2.743
358highlands	452.734	6.040	1.010	0.410	4.506	3.496

References

Cabrol, N., G. Edmond, M. Carr, B. Sutter, J. Moore, J. Farmer, R. Greenley, R. Kuzmin, D. DesMarais, M. Kramer, H. Newsom, C. Barber, I. Thorsos, K. Tanaka, N. Barlow, D. Fike, M. Urquhart, B. Grisby, F. Grant, O. de Goursac, *J. Geophys. Res.*, 108 (E12): doi:10.1029/2002JE002026, 2003.

Christensen, E. and W. Hamblin, Exploring the Planets (1995), (2nd Edition), Prentice-Hall.

Frey, H., S. Sakimoto, J. Roark, *Geophys. Res. Lett.* 26, No. 12, Pages 1657-1660, June 15, 1999.

Frey, H., S. Sakimoto, J. Roark, Discovery of a New Cassini-Size Basin on Mars from MOLA Topographic Data, *Lunar and Planet. Sci. XXX*, Abstract 1497, 1999.

Frey, H., J. Roark, K. Shockey, E. Frey, S. Sakimoto, *Geophys. Res. Lett.* 29, No. 10, 1384, 10.1029/2001GL013832, 2002.

Garvin and Frawley, Geometric properties of Martian impact craters: Preliminary results from Mars Orbiter Laser Altimeter, *Geophys. Res. Lett.* 25:4405-4408, 1998.

Gellert, R., J. Brückner, B. Clark, G. Dreibus, C. d'Uston, T. Economou, G. Klingelhöfer, G. Lugmair, D. Ming, R. Morris, R. Rieder, S. Squyres, H. Wänke, A. Yen, J. Zipfel, Chemical Diversity Along the Traverse of the Rover Spirit at Gusev Crater (abstract), *Lunar Planet. Sci. Conf. XXXVII*, Abstract #2176, Lunar and Planetary institute, Houston, TX (CD-ROM), 2006.

Herrick and Forsberg-Taylor, *Meteoritics & Planetary Science*, 38, Nr 11, 155-1578, 2003.

Howenstine and Kiefer, *20th Annual Summer Intern Conference*, Lunar and Planetary Institute, Houston, Texas, August 12, 2004.

Kiefer, Walter, *Lunar Impact Crater Geology and Structure*, website, 2001: http://www.lpi.usra.edu/expmoon/science/craterstructure.html

Lane, M., M. Dyar, J. Bishop, *Geophys. Res. Lett.* 31, L19702, doi:10.1029/2004GL021231, 2004.

Leonard and Tanaka, *USGS Geologic Map*, I-2694, 2001.

Martinez-Alonzo, S., B. Jakosky, M. Mellon, N. Putzig, *J. Geophys. Res.*, 110 (E01003): doi: 10.1029/2004JE002327, 2005.

Monders, A., E. Médard, T. Grove, Basaltic Lavas at Gusev Crater Revisited (abstract), *Lunar Planet. Sci. Conf. XXXVII*, Abstract #1834, Lunar and Planetary Institute, Houston, TX (CD-ROM), 2006.

Morris, R. V., G. Klingelhöfer, B. Bernhardt, C. Schröder, D. S. Rodionov, P. A. de Souza, Jr., A. Yen, R. Gellert, E. N. Evlanov, J. Foh, E. Kankeleit, P. Gütlich, D. W. Ming, F. Renz, T. Wdowiak, S. W. Squyres, and R. E. Arvidson, 2004, Mineralogy at Gusev Crater from the Mössbauer Spectrometer on the Spirit Rover, *Science*, 305(5685), 833-836, doi:10.1126/science.1100020.

Pike, *Impact and Explosion Cratering*, 489-509, 1977.

Roark, J., H. Frey, S. Sakimoto, Interactive graphics tools for analysis of MOLA and other data (abstract), *Lunar Planet. Sci. Conf. XXXI*, Abstract #2026, Lunar and Planetary institute, Houston, TX (CD-ROM), 2000.

Roark, J. C. Masuoka, H. Frey, Gridview: Recent Improvements in Research and Education Software for Exploring Mars Topography, *Lunar and Planetary Science 35*, abstract: 1833, 2004.

Schultz, P., R. Schultz, J. Rogers, The Structure and Evolution of Ancient Impact Basins on Mars, *J. Geophys. Res.*, Vol. 87, No. B12, Pages 9803-9820, November 30, 1982.

Schultz and Frey, A New Survey of Multiring Impact Basins on Mars, *J. Geophys. Res.*, 95, No. B9, Pages 14,175-12,189, August 30, 1990.

Smith, D., M. Zuber, H. Frey, J. Garvin, J. Head, D. Muhleman, G. Pettengill, R. Phillips, S. Solomon, H. Zwally, W. Banerdt, T. Duxbury, M. Golombek, F. Lemoine, G. Neumann, D. Rowlands, O. Aharonson, P. Ford, A. Ivanov, C. Johnson, P. McGovern, J. Abshire, R. Afzal, X. Sun, *J. Geophys. Res.* 106:23,689-23,722, 2001.

Strom R.G., S. K. Croft, and N. G. Barlow (1992). The Martian impact cratering record. In *Mars* (H.H. Kieffer, B.M. Jakosky, C.W. Snyder, and M.S. Matthews, eds.). Univ. Arizona Press, Tucson, AZ, pp. 383-423.

Tanaka, K.L., The stratigraphy of Mars. Proceedings of the 17th Lunar and Planetary Science Conf., Part 1. Journal of Geophysical Research, 91, supplement, E139-E158, 1986.

USGS List, *Mars System Nomenclature*, United States Geologic Survey, March 14, 2006: http://planetarynames.wr.usgs.gov/jsp/SystemSearch2.jsp?System=Mars

Williams, K., M. Zuber, Measurement and Analysis of Lunar Basin Depths from Clementine Altimetry, *Icarus* 131, 107-112 (1998), Article No. IS975856.